



ELSEVIER

Contents lists available at ScienceDirect

Applied Radiation and Isotopes

journal homepage: www.elsevier.com/locate/apradiso

Technical note

Radiosynthesis and *in vivo* evaluation of a ^{18}F -labelled styryl-benzoxazole derivative for β -amyloid targeting

G. Ribeiro Morais^a, L. Gano^a, T. Kniess^b, R. Bergmann^b, A. Abrunhosa^c, I. Santos^a, A. Paulo^{a,*}

^a Radiopharmaceutical Sciences Group, IST/ITN, Instituto Superior Técnico, Universidade Técnica de Lisboa, EN 10, 2686-953 Sacavem, Portugal

^b Institute of Radiopharmaceutical Cancer Research, Helmholtz-Zentrum Dresden-Rossendorf e.V., POB 510119, D-01314 Dresden, Germany

^c Universidade Coimbra, ICNAS, Inst Nucl Sci Appl Saúde, P-3000 Coimbra, Portugal

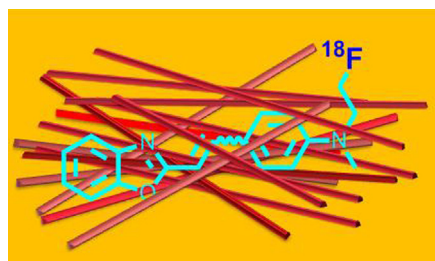


HIGHLIGHTS

- Design of a fluorinated styryl benzoxazole derivative for detection of β -amyloid plaques.
- Nucleophilic radiofluorination with readily available [^{18}F]KF.
- Metabolism and biodistribution studies of the radiofluorinated styryl benzoxazole derivative.

GRAPHICAL ABSTRACT

A New ^{18}F -Labeled Styryl Benzoxazole Derivative (^{18}F -**1**) for β -Amyloid Targeting has been synthesized in good radiochemical yield and high radiochemical purity (> 99%, both isomers). Biodistribution and metabolism studies of ^{18}F -**1** in male Wistar rats have shown that this new radiotracer can cross the BBB but has a poor *in vivo* stability.



ARTICLE INFO

Article history:

Received 9 January 2013

Received in revised form

15 April 2013

Accepted 1 July 2013

Available online 13 July 2013

Keywords:

Alzheimer's Disease
 β -Amyloid aggregation
 Molecular imaging
 Fluorine-18

ABSTRACT

The formation of β -amyloid deposits is considered a histopathological feature of Alzheimer's disease (AD). *In vivo* molecular imaging by means of amyloid-avid radiotracers will allow for an early and conclusive diagnostic of AD. Herein, we describe the radiosynthesis of the radiofluorinated styryl benzoxazole derivative [^{18}F]-[2-[N-methyl-N-(2'-fluoroethyl)-4'-aminostyryl]benzoxazole] (^{18}F -**1**) and its pre-clinical evaluation, including metabolic and biodistribution studies in male Wistar rats. The *in vivo* biological evaluation of ^{18}F -**1** showed that this new radiotracer has a moderate brain uptake with a slow brain washout and a poor *in vivo* stability.

© 2013 Elsevier Ltd. All rights reserved.

1. Introduction

Progressive neurodegenerative disorders such as Alzheimer's (AD) or Parkinson's (PD) disease affect millions of persons worldwide and pose a significant impact in public health, especially as more people approach old age. These diseases, known as "protein misfolding diseases" are characterized by the accumulation of insoluble protein

deposits like β -amyloid ($\text{A}\beta$), neurofibrillar tangles in AD, and alpha-synuclein (αSyn) in PD. The molecular processes underlying these diseases are still not completely understood, but the deposition of the amyloid deposits is considered an early and specific event in their pathogenesis (Bacsikai et al., 2003; Irvine et al., 2008).

Being available suitable probes for *in vivo* targeting of $\text{A}\beta$ deposits, the use of molecular imaging modalities is expected to demonstrate the locations and densities of such deposits in the AD brain allowing an early and assertive diagnosis of AD and/or the monitoring of anti-amyloidogenic therapies. Among the available molecular imaging modalities, positron emission tomography

* Corresponding author. Tel.: +351219946196.
 E-mail address: apaulo@itn.pt (A. Paulo).

(PET) is the best suited to achieve such goal, particularly based on amyloid-avid molecules radiolabelled with the cyclotron produced radionuclides carbon-11 (^{11}C) and fluorine-18 (^{18}F) (Kung, 2012; Lee et al., 2012; Ribeiro Morais et al., 2012).

A good performing PET radiotracer for *in vivo* imaging of amyloid deposits must show a high binding affinity to $\text{A}\beta$ and a good permeability through the blood brain barrier (BBB), with minimal non-specific retention in the brain. Taking these requisites into consideration, a plethora of small-sized, planar and non-ionic ^{11}C - and ^{18}F -labelled molecules have been synthesized and evaluated as radiotracers for *in vivo* detection of $\text{A}\beta$ deposits in AD-affected brain. From these studies, the Pittsburgh compound B (^{11}C]PIB) (Fig. 1) emerged as the gold standard PET radiotracer for *in vivo* β -amyloid imaging (Klunk et al., 2004). However, the short-life of ^{11}C ($t_{1/2}=20.4$ min) limits its use to centers with an on-site cyclotron. Hence, an intense research effort has been done to obtain alternative ^{18}F -based radioprobes, as the longer half-life ($t_{1/2}=110$ min) of ^{18}F allows for multistep radiosynthesis, longer *in vivo* investigation, and commercial distribution to other clinical PET centers. In recent years, encouraging results have been reported for a few ^{18}F -labeled compounds (Fig. 1) (Liu et al., 2007; Choi et al., 2009; Jureus et al., 2010; Vandenberghe et al., 2010; Barthel et al., 2011; Clark et al., 2011) that underwent clinical evaluation in humans as $\text{A}\beta$ imaging agents. One of these agents, ^{18}F -Florbetapir (Amyvid) has been recently approved by the FDA for clinical use, giving *in vivo* PET images of amyloid deposits in close correlation with results from postmortem histopathological analysis (Clark et al., 2011).

Despite this success, there is still room to investigate alternative PET radioprobes for *in vivo* detection of amyloid aggregates, aiming at the finding of best performing compounds with augmented initial brain uptake and with reduced non-specific retention in the brain. For this purpose, we have designed a novel family of fluorinated styryl benzoxazole derivatives that interact *in vitro* with amyloid species in the same way as does Thioflavin T, which is a dye used to stain $\text{A}\beta$ deposits in post-mortem histopathological studies. In this paper, we report on the radiosynthesis of one of these compounds, [^{18}F]-2-[N-methyl-N-(2'-fluoroethyl)-4'-aminostyryl] benzoxazole ([^{18}F]-1), as well as on its *in vivo* evaluation that comprised biodistribution and metabolism studies in rat.

2. Experimental section

2.1. Chemistry

The tosylated precursor 2-[N-methyl-N-(2'-tosyloxyethyl)-4'-aminostyryl]benzoxazole (**3**) and the cold surrogate 2-[N-methyl-N-(2'-fluoroethyl)-4'-aminostyryl]benzoxazole (**1**) were synthesized

according to previously reported (Ribeiro Morais et al., 2011). Briefly, 2-benzoxazolylmethyltriphenylphosphonium chloride (2.0 g, 4.6 mmol) in benzene (25 mL) was reacted with K^tBuO (525 mg, 4.7 mmol) at rt. After 3 h, the reaction mixture was diluted with EtOAc (100 mL) and was extracted with water (100 mL). The organic phase was dried over MgSO_4 , filtered and the filtrate was dried under vacuum. Then, the resulting phosphorane was refluxed overnight with *N*-methyl-*N*-(2-tosyloxyethyl)-4 aminobenzaldehyde (590 mg, 1.8 mmol) in anhydrous THF (25 mL). Thereafter, the solvent was concentrated and the reaction crude was re-dissolved in CH_2Cl_2 (100 mL). The organic phase was extracted with sat. sol. of NaHCO_3 (100 mL). The organic extract was dried over MgSO_4 , filtered and the filtrate was concentrated. Compound **3** (550 mg, 65%) was purified by column chromatography on silica gel (*n*-hexane/EtOAc/ CHCl_3 3:1:1). To a solution of **3** (250 mg, 0.55 mmol) in anhydrous THF (23 mL) was added anhydrous TBAF (1.8 mL, 1.8 mmol, 1.0 M in THF). The reaction mixture was refluxed for 30 minutes. Thereafter the solvent was concentrated; chloroform (50 mL) was added to the residue and was extracted with sat sol NaHCO_3 (50 mL). The organic phase was dried over MgSO_4 , filtered and the filtrate was concentrated. Column chromatographic on silica gel (*n*-hexane/EtOAc 4:1) gave the mixture of **1-Z** and **1-E** (124 mg, 76%).

2.2. Radiochemistry

No-carrier-added aqueous [^{18}F]fluoride was produced in a CYCLONE 18/9 cyclotron (IBA) by irradiation of [^{18}O]H $_2\text{O}$ via the $^{18}\text{O}(\text{p},\text{n})^{18}\text{F}$ nuclear reaction. Resolubilization of the aqueous [^{18}F] fluoride (0.8–1.0 GBq) was accomplished as described by Coenen et al. (Coenen et al., 1986) with Kryptofix[®] 2.2.2 and K_2CO_3 in a conical vial and azeotropically removing water with acetonitrile in a stream of nitrogen. Finally the dried [^{18}F]KF was resolubilized in 500 μL of anhydrous acetonitrile and added to **3** (3.0 mg) in a conical glass vial. The vial was sealed and heated for 20 min at 90 °C in an oil bath. After cooling the mixture was subjected to semi-preparative HPLC (Discovery C18, 4.6 \times 250 mm, 5 μm , Supelco) using isocratic elution with acetonitrile/0.1%TFA (70/30) at a flow rate of 4 mL/min originated by a PU1580 pump (Jasco). The products were monitored by UV detector (UV2075, Jasco) at 254 nm and by *gamma*-detection with a scintillation detector (Nuclear Interface).

The radiolabeled product [^{18}F]-**1** eluting at 9–10 min was separated, diluted with 30 mL of water and the whole solution was subjected to a C18 cartridge (200 mg, LiChrolut). The cartridge was washed with 5 mL of water, after that the radiolabeled product [^{18}F]-**1** was eluted with 1 mL of ethanol and reconstituted with 8 mL of E153 electrolyte infusion solution (140 mmol/L Na^+ , 5 mmol/L K^+ , 2.5 mmol/L Ca^{++} , 1.5 mmol/L Mg^{++} , 50 mmol/L

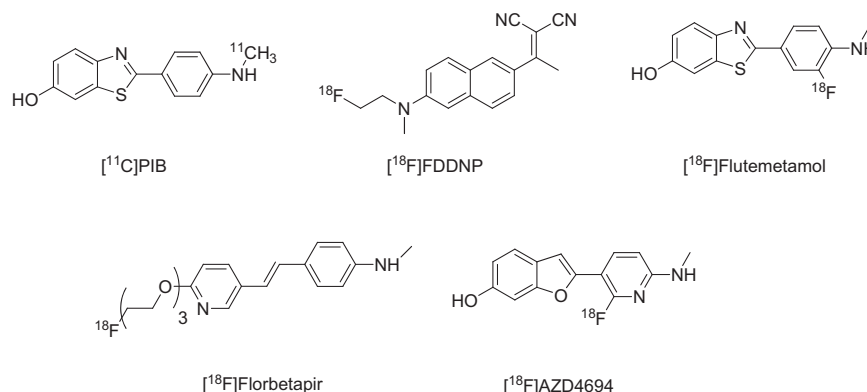


Fig. 1. Chemical structure of relevant $\text{A}\beta$ binding agents.

acetate, 103 mmol/L Cl⁻, Serumwerk Bernburg AG, Bernburg, Germany). This solution was used for biodistribution experiments and stability studies.

Analytical HPLC analyses of the radiolabeled product [¹⁸F]-**1** were performed by a Lichrograph[®] system (Merck–Hitachi) equipped with a L4500 UV detector, a L6200 pump and a scintillation detector Gabi (Raytest) using a C18 column (Luna C18(2), 4.6 × 250, 5 μm) and the indicated isocratic eluent with a flow rate of 1.0 mL/min.

The radiotracer [¹⁸F]-**1** was synthesized in 70 min total synthesis time in 42% total decay corrected yield from [¹⁸F]fluoride in > 99% radiochemical purity (both isomers) and a specific activity 7–28 GBq/μmol at end of synthesis.

2.3. Metabolite analysis

Male Wistar-Unilever rats ($n=2$; body weight 150 ± 12 g) were anesthetized with desflurane (9–10% v/v, 30% oxygen/air). The threshold value for breathing frequency was 65 breaths/min. Animals were put in supine position and placed on a heating pad to maintain body temperature. The spontaneously breathing rats were heparinized with 100 units/kg heparin (Heparin-Natrium 25.000-ratiopharm[®], ratiopharm GmbH, Germany) by subcutaneous injection to prevent blood clotting on intravascular catheters. After local anesthesia with lignocain (1%; Xylocitin[®] loc, mibe, Jena, Germany) into the right groin, a catheter (0.8 mm Umbilical Vessel Catheter, Tyco Healthcare, Tullamore, Ireland) was introduced into the right femoral artery for arterial blood sampling. A second needle catheter (35 G) was placed into a tail vein and was used for [¹⁸F]-**1** radiotracer injection (39 MBq in 0.5 mL of E153/10% ethanol, infusion 1 mL/min). Arterial blood samples were taken 1.5, 10, 30 and 60 min after injection. Arterial plasma was separated by centrifugation ($11.000g \times 3$ min) followed by precipitation of the proteins with methanol (2 volumes to 1 volume plasma) followed by 5 min storage at -60 °C. The clear supernatant separated by centrifugation was used for analysis. The radio-HPLC system (Agilent 1100 series) applied for metabolite analysis was equipped with UV detection (254 nm) and an external radiochemical detector (RAMONA, Raytest GmbH, Straubenhardt, Germany). Analysis was performed on a Zorbax C18 300SB (250 × 9.4 mm; 4 μm) column with an eluent system A (water+0.1%TFA) and B (acetonitrile+0.1% TFA) in the following gradient: 5 min 95% A, 10 min to 95% B, 5 min at 95% B and 5 min to 95%A at a flow rate of 3 mL/min.

2.4. Biodistribution studies in Wistar rats

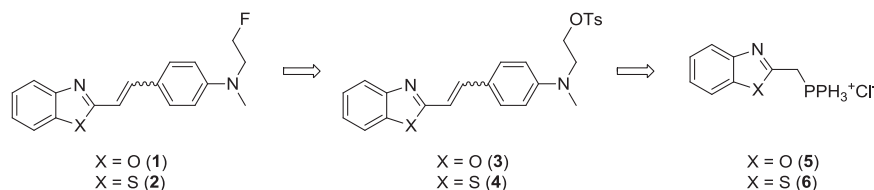
The animal research committee of the Regierungspräsidium Dresden approved the animal facilities and the experiments according to institutional guidelines and the German animal welfare regulations. The experimental procedure used conforms to the *European Convention for the Protection of Vertebrate Animals used for Experimental and other Scientific Purposes* (ETS No. 123), to the *Deutsches Tierschutzgesetz*, and to the *Guide for the Care and Use of Laboratory Animals* published by the US National Institutes of Health (DHEW Publication No. (NIH) 82–23, Revised 1996, Office

of Science and Health Reports, DRR/NIH, Bethesda, MD 20205). The Wistar rats (Wistar Unilever, HsdCpb: Wu, Harlan Winkelmann GmbH, Borcheln, Germany, 138 ± 16 g body weight) were housed under standard conditions with free access to standard food and tap water. The biodistribution of [¹⁸F]-**1** was studied in 7 male rats at 5 min and 8 male rats at 60 min after tracer injection. The animals were anesthetized with Desflurane (Suprane, Baxter Healthcare Corporation Deerfield, IL, USA) (7.0–10.0% v/v in 30% oxygen) and 3–5 MBq radiotracer aliquots were administered in 500 μL electrolyte solution E153 (with 10% ethanol) and into a tail vein. After recovery from anaesthesia rats were again anaesthetized at 5 or 60 min after tracer injection, respectively. Blood was withdrawn by heart puncture, and the animals were euthanized. Organs and tissues were removed, dried, weighted, and the radioactivity was measured in a cross calibrated well counter (WIZARD, Automatic Gamma Counter, Perkin Elmer, Waltham, Ma, USA) or activimeter (Activimeter Isomed 2000; MCD Nuklear Medizintechnik, Dresden, Germany). The data were decay corrected and normalized to the amount of injected activity calculated from the activity of injection syringes before and after injection and expressed as percentage of injected activity (%ID) or injected activity per gram of tissue (%ID/g). Values are quoted as means ± standard deviation (mean ± SD) for a group of animals.

3. Results and discussion

Recently, we have introduced new fluorinated styryl benzoxazole (compound **1**) and styryl benzothiazole (compound **2**) derivatives that were synthesized based on a multistep and convergent approach, using the Wittig reaction as a key step to introduce the styryl moiety (Scheme 1) (Ribeiro Morais et al., 2011). Compounds **1** and **2** were obtained as mixtures of geometric *E* and *Z* isomers, being the *E* isomer formed preferably in spite of the *Z/E* photoisomerization ability of these compounds. The assessment of the *in vitro* binding affinity of the *E* and *Z* isomers of **1** and **2** towards different types of amyloid fibrils (insulin, α-synuclein and β-amyloid peptide) has shown that compound **1** displays the highest Aβ binding affinity and selectivity. These studies have also proved that the *Z/E* geometric isomerism has almost no influence on the binding profile of **1** and **2** (Ribeiro Morais et al., 2011). Altogether, these data led us to consider **1** the most promising compound to be further evaluated as an amyloid-avid probe for *in vivo* detection of Aβ deposits. Hence, we have studied the synthesis of the ¹⁸F-labelled counterpart ([¹⁸F]-**1**) of compound **1** and proceeded with its *in vivo* biological evaluation, as reported in here.

The radiosynthesis of the ¹⁸F-labelled styryl benzoxazole ([¹⁸F]-**1**) has been done using the tosylated precursor **3** as starting material, using a synthetic methodology similar to that previously reported to obtain the cold congener (**1**) (Ribeiro Morais et al., 2011). The optimization of the radiosynthesis involved the study of the influence of the temperature (80–100 °C) and use of different solvents (dimethylformamide vs acetonitrile). Under optimized conditions, the synthesis of [¹⁸F]-**1** was achieved by nucleophilic displacement of the tosylate group with dried K[¹⁸F] at 90 °C for 20 min, using acetonitrile as solvent and K₂.2.2/K₂CO₃ to catalyze



Scheme 1. Retrosynthetic approach for the preparation of fluorinated styryl benzazoles (Ribeiro Morais et al., 2011).

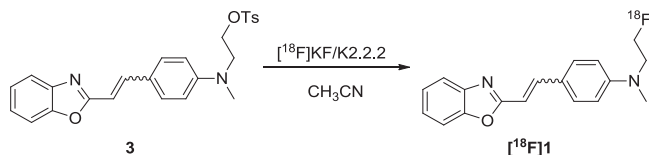
the reaction (Scheme 2). This combination catalyst, commonly used in radiofluorination reaction, increases the solubility of the fluoride ion and enhances its nucleophilicity (Liu et al., 2010). The radiotracer [^{18}F]-1 has been purified by semipreparative HPLC using an isocratic elution with acetonitrile/0.1% TFA (70/30). After HPLC purification, [^{18}F]-1 has been obtained as a mixture of the two *E* and *Z* isomers, as confirmed by HPLC (Fig. 2). No efforts have been made to separate the two *E* and *Z* isomers of [^{18}F]-1 since they have the similar affinity towards $\text{A}\beta(1-42)$ aggregates with binding constants of 4.48 ± 0.38 and $5.99 \pm 0.56 \mu\text{M}^{-1}$, respectively (Ribeiro Morais et al., 2011). Prior to the biodistribution experiments and stability studies, [^{18}F]-1 has been reformulated into an aqueous solution containing 10% of ethanol, using a solid phase extraction (SPE) C18 cartridge to perform the reformulation. [^{18}F]-1 was synthesized in an overall 42% decay-corrected radiochemical yield and high radiochemical purity (> 99%, both isomers) with a specific activity of 7–28 GBq/ μmol at end of synthesis. The radiotracer [^{18}F]-1 was synthesized in 70 min total synthesis time, which included the purification and reformulation. The radiochemical purity was determined based on radio-TLC and analytical HPLC experiments. The chemical identity of compound [^{18}F]-1 was assessed by HPLC comparison with authentic samples of the *E* and *Z* isomers of the cold congener 1.

Biodistribution and metabolism studies of [^{18}F]-1 were performed in male Wistar rats, in order to have a first insight into its potential relevance as a radiotracer for *in vivo* imaging of $\text{A}\beta$ aggregates. In particular, these studies intended to elucidate if the compound could cross the BBB with a fast washout from the

healthy brain, a crucial issue to reach intra cerebral amyloid deposits with minimal non-specific uptake.

The biodistribution data of [^{18}F]-1 in male Wistar rats are presented in Table 1. The data were obtained at 5 and 60 min post-injection (p.i), after intravenous bolus injection of the radiotracer. At early post-injection times, it was observed a moderately fast clearance of the ^{18}F -radioactivity from the blood compartment with a value of $0.49 \pm 0.20\%$ ID/g at 5 min p.i. The percentages of injected dose (ID) that were found in the liver ($4.83 \pm 2.16\%$ at 5 min p.i. and $2.38 \pm 0.28\%$ at 60 min p.i.) and intestine ($5.30 \pm 2.63\%$ at 5 min p.i. and $13.66 \pm 1.90\%$ at 60 min p.i.) indicate a significant contribution of hepatobiliary excretion, as expected for a lipophilic compound. [^{18}F]-1 presents a calculated octanol/water partition coefficient ($\log P_{o/w}$) of 4.01, as we have reported previously (Ribeiro Morais et al., 2011). [^{18}F]-1 has shown a moderate initial brain uptake ($0.61 \pm 0.26\%$ ID/g at 5 min p.i.), which is consistent with its lipophilicity. The activity retained in the brain was $0.45 \pm 0.04\%$ ID/g, 60 min after i.v. administration (Fig. 3). Therefore, [^{18}F]-1 undergoes a relatively slow brain washout (5-to-60 min ratio = 1.36) in normal rat, which is a non favorable behavior for a specific radioprobe targeted at $\text{A}\beta$ aggregates. In addition, [^{18}F]-1 showed a significant femur uptake ($0.50 \pm 0.21\%$ ID/g at 5 min p.i.; $0.75 \pm 0.13\%$ ID/g at 60 min p.i.) that increased with time (Fig. 3), indicating the occurrence of *in vivo* defluorination. *In vivo* defluorination has been recently reported for related ^{18}F -labeled styryltriazone derivatives carrying also the radioactive label at an aliphatic sp³ carbon atom (Lee et al., 2012).

The observed slow brain washout and increasing femur uptake indicated that [^{18}F]-1 was not stable *in vivo*, undergoing probably



Scheme 2. Synthesis of [^{18}F]-1 using aliphatic nucleophilic radiofluorination.

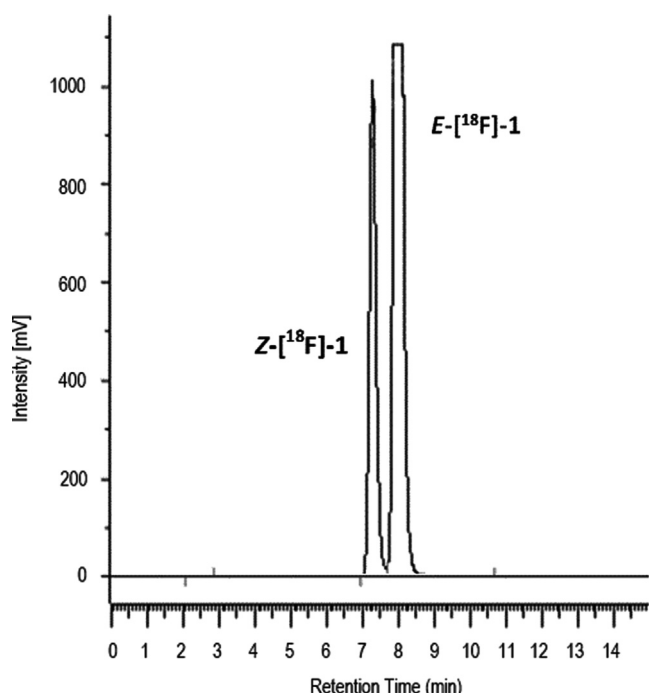


Fig. 2. HPLC profile compound [^{18}F]-1 (radiometric detection) with the assignment of its *E* and *Z* isomers.

Table 1

Biodistribution results of [^{18}F]-1 in male Wistar rat at 5 and 60 min after i.v. administration, expressed in %ID/organ \pm SD or %ID/g tissue \pm SD ($n=7-8$).

Organ	% ID		%ID/g	
	5 min p.i.	60 min p.i.	5 min p.i.	60 min p.i.
Blood			0.49 ± 0.19	0.56 ± 0.08
Hair and skin			0.33 ± 0.15	0.35 ± 0.06
Brain	0.92 ± 0.39	0.68 ± 0.08	0.60 ± 0.25	0.44 ± 0.06
Pancreas	0.12 ± 0.04	0.08 ± 0.01	0.53 ± 0.15	0.32 ± 0.06
Spleen	0.14 ± 0.06	0.10 ± 0.01	0.54 ± 0.24	0.37 ± 0.07
Adrenals	0.05 ± 0.01	0.03 ± 0.01	1.28 ± 0.43	0.88 ± 0.16
Kidneys	0.82 ± 0.28	0.56 ± 0.04	0.76 ± 0.23	0.49 ± 0.08
Muscle			0.32 ± 0.14	0.28 ± 0.04
Heart	0.26 ± 0.07	0.24 ± 0.02	0.57 ± 0.15	0.51 ± 0.09
Lung	0.50 ± 0.15	0.38 ± 0.03	0.70 ± 0.20	0.51 ± 0.08
Thymus	0.31 ± 0.15	0.27 ± 0.03	0.87 ± 0.44	0.71 ± 0.18
Liver	4.82 ± 2.15	2.38 ± 0.27	0.98 ± 0.43	0.50 ± 0.08
Femur	0.34 ± 0.14	0.52 ± 0.04	0.49 ± 0.21	0.74 ± 0.12
Testes	0.28 ± 0.13	0.44 ± 0.06	0.14 ± 0.07	0.22 ± 0.03
Intestine	5.30 ± 2.62	13.66 ± 1.89		
Stomach	0.52 ± 0.42	0.44 ± 0.12		

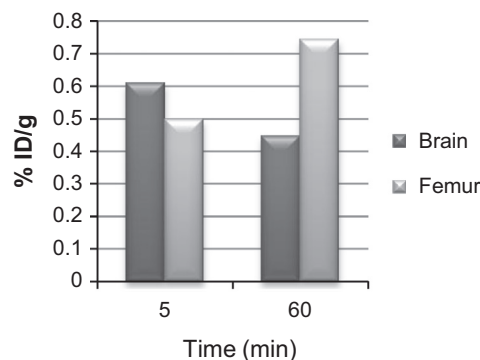


Fig. 3. Brain and femur uptake of [^{18}F]-1 as a function of time.

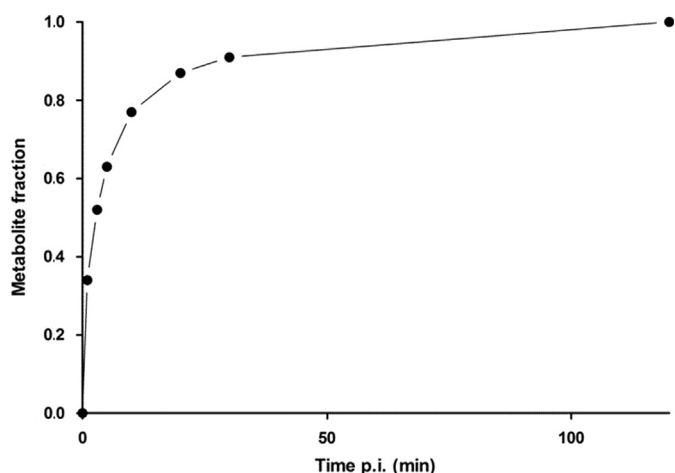


Fig. 4. Metabolite fraction in the blood plasma from a Wistar rat injected with $[^{18}\text{F}]\text{-1}$.

defluorination processes. To have a further insight into this point, we have performed radio-HPLC analysis of blood plasma from Wistar rats injected with $[^{18}\text{F}]\text{-1}$. This study confirmed that $[^{18}\text{F}]\text{-1}$ was rapidly metabolized into a polar metabolite (see Supporting Information), being depicted in Fig. 4 the variation of the metabolite fraction over time. After 30 min p.i., the plasma activity was due almost exclusively to the metabolite, which indicates that $[^{18}\text{F}]\text{-1}$ has a poor *in vivo* stability.

4. Conclusions

A novel radiofluorinated styryl-benzoxazole derivative ($[^{18}\text{F}]\text{-1}$) targeted at $\text{A}\beta$ aggregates has been synthesized in good yield and with high radiochemical purity and specific activity. Biodistribution and metabolism studies in rat have shown that this newly synthesized radiotracer can cross the BBB but displays a rather slow brain washout. Moreover, $[^{18}\text{F}]\text{-1}$ suffers extensive metabolism/defluorination *in vivo* and, therefore, is not a suitable radioprobe for *in vivo* imaging of $\text{A}\beta$ deposits in AD-affected brain. To overcome these drawbacks, we envisage to explore the use of different aliphatic linkers between the $-\text{CH}_2^{18}\text{F}$ group and the phenyl ring, as it has been reported that such linkers can strongly influence the *in vivo* stability of this type of compounds (Lee et al., 2012).

Acknowledgments

This work was funded by Fundação para a Ciência e Tecnologia (FCT), Portugal (PTDC/QUI/102049/2008). GRM thanks the FCT for the ‘Ciência 2008’ program and DAAD program (0811983). The research was carried out within the framework of the European Cooperation COST Action TD1007 (Bimodal PET-MRI molecular imaging technologies and applications for *in vivo* monitoring of disease and biological processes).

References

- Bacskai, B.J., Hickey, G.A., et al., 2003. Four-dimensional multiphoton imaging of brain entry, amyloid binding, and clearance of an amyloid-beta ligand in transgenic mice. *Proc. Nat. Acad. Sci. U.S.A.* 100 (21), 12462–12467.
- Barthel, H., Gertz, H.J., et al., 2011. Cerebral amyloid-beta PET with florbetaben (F-18) in patients with Alzheimer’s disease and healthy controls: a multicentre phase 2 diagnostic study. *Lancet Neurol.* 10 (5), 424–435.
- Choi, S.R., Golding, G., et al., 2009. Preclinical properties of F-18-AV-45 : a PET agent for a beta plaques in the brain. *J. Nucl. Med.* 50 (11), 1887–1894.
- Clark, C.M., Schneider, J.A., et al., 2011. Use of florbetapir-PET for imaging beta-amyloid pathology. *JAMA* 305 (3), 275–283.
- Coenen, H.H., Klatte, B., et al., 1986. J. Labelled Compd. Radiopharm. 23, 455–463.
- Irvine, G.B., El-Agnaf, O.M., et al., 2008. Protein aggregation in the brain: the molecular basis for Alzheimer’s and Parkinson’s diseases. *Mol. Med.* 14 (7–8), 451–464.
- Jureus, A., Swahn, B.M., et al., 2010. Characterization of AZD4694, a novel fluorinated A beta plaque neuroimaging PET radioligand. *J. Neurochem.* 114 (3), 784–794.
- Klunk, W.E., Engler, H., et al., 2004. Imaging brain amyloid in Alzheimer’s disease with Pittsburgh Compound-B. *Ann. Neurol.* 55 (3), 306–319.
- Kung, H.F., 2012. The beta-amyloid hypothesis in Alzheimer’s disease: seeing is believing. *ACS Med. Chem. Lett.* 3 (4), 265–267.
- Lee, I., Choe, Y.S., et al., 2012. Synthesis and evaluation of F-18 -labeled styryltriazone and resveratrol derivatives for beta-amyloid plaque imaging. *J. Med. Chem.* 55 (2), 883–892.
- Liu, J., Kepe, V., et al., 2007. High-yield, automated radiosynthesis of 2-(1-[(2-[F-18]fluoroethyl)(methyl)amino]-2-naphthyl)ethylidene)malononitrile(F-18) FDDNP) ready for animal or human administration. *Mol. Imaging Biol.* 9 (1), 6–16.
- Liu, Y.J., Zhu, L., et al., 2010. Optimization of automated radiosynthesis of $[\text{F-18}]\text{-AV-45}$: a new PET imaging agent for Alzheimer’s disease. *Nucl. Med. Biol.* 37 (8), 917–925.
- Ribeiro Morais, G., Miranda, H.V., et al., 2011. Synthesis and *in vitro* evaluation of fluorinated styryl benzazoles as amyloid-probes. *Bioorg. Med. Chem.* 19 (24), 7698–7710.
- Ribeiro Morais, G., Paulo, A., et al., 2012. A synthetic overview of radiolabeled compounds for ss-amyloid targeting. *Eur. J. Org. Chem.* 7, 1279–1293.
- Vandenbergh, R., Van Laere, K., et al., 2010. F-18 -Flutemetamol amyloid imaging in Alzheimer disease and mild cognitive impairment A Phase 2 trial. *Ann. Neurol.* 68 (3), 319–329.